A COMPARISON OF NUMERICAL SIMULATIONS AND FULL-SCALE MEASUREMENTS OF SNOWDRIFTS AROUND BUILDINGS

Thomas K. Thiis, Narvik Institute of Technology,

p.b. 385, N-8501 Narvik, Norway, e-mail: tht@hin.no

Snowdrifts around buildings can cause serious problems when formed on undesirable places. The formation of snowdrifts is highly connected to the wind pattern around the building, and the wind pattern is again dependent on the building design. The shear stress on the surface and snowdrifting around different buildings are investigated through CFD analysis and compared to measurements. The computations of shear stress shows local minima in the same areas as snowdrifts are formed. The snowdrifting computations utilises a drift-flux model where a fluid with snow properties is allowed to drift through a fluid with air properties. An apparent dynamic viscosity of the snow/air mixture is defined and used as a threshold criterion for snowdrifting. The results from the snowdrifting computations show increased snow density where snowdrifts are expected, and are in agreement with previous large-scale snowdrift measurements. The results show that computational fluid dynamics can be a tool for planning building design in snowdrifting areas.

INTRODUCTION

Snowdrift formation around buildings can be a major problem in snowy and windy areas. The planning of buildings in such areas should therefore also consider the position of snowdrifts in respect to outdoor facilities such as doors, roads and car sheds. The snowdrifts deposited around a building in a windy area are usually more a result of wind transported, redistributed snow particles, and not so much a result of free falling precipitation. Thus the wind pattern around a building is of high importance to both the spatial distribution of blowing snow particles and the deposition of the particles around the building.

The transportation of snow can occur in three different modes; creep - rolling particles near the ground, saltation - jumping particles some centimetres above the ground and suspension - free flying particles ten folds of meters above the ground. The mode present depends on the ratio of particle

weight to wind force exerted on the particle, though saltation and creep must occur before suspension takes place, and saltation is initiated first when creep is occurring. The transport rate of creeping particles is in this connection negligible. Since most of the depositing or eroding particles is near the surface, it is mainly the physical mechanisms of saltation which is most interesting for the formation of snowdrifts around obstacles. The transport rate of saltating snow, defined as the mean saltating mass crossing a lane of unit width at some mean velocity is expressed

$$Q_s = u_p W_p / g \qquad \text{[kg/m•s]} \qquad (1)$$

where u_p is the mean particle velocity, W_p is the mean weight of saltating snow and g is the accleration due to gravity. The weight of the saltating snow, W_p, is related to the magnitude of the flow shear stress applied to the particle by

$$W_p = e(\tau - \tau_t) \qquad \text{[N/m}^2\text{]} \qquad (2)$$

(Pomeroy and Gray, 1990). Here e is the efficiency of saltation and has the range 0-1. e is inversely related to the kinetic energy resulting from particle impact, rebound, and ejection of scattered crystals at the snow surface. τ is the total atmospheric shear stress and τ_t is the shear stress applied to erodible surfaces. τ_t is equivalent to the shear stress required to maintain particle ejection and is also approximately the total atmospheric shear stress at which particle ejection is assumed to cease (Owen, 1964). For this case,

$$\tau_t = \rho u_{*t}^2 \qquad \text{[N/m}^2\text{]} \qquad (3)$$

where u_{*t} is the threshold friction velocity. The value of u_{*t} is related to the physical properties of the snow and is ranging from 0.07 to 0.25 m/s for fresh, dry snow and from 0.25 to 1 m/s for old, wind hardened snow (Kind, 1981). From this it can be assumed that if there are saltating particles over a surface, and the atmospheric shear stress on a limited area suddenly drops below the threshold shear stress for saltation, accumulation of snow particles is occurring on that area.

The concentration of blowing snow in the air has been studied by Mellor and Fellers (1986), and based on multiple regression analysis on data collected in Antarctica, they found that over a uniform surface, the mass concentration of snow can be expressed by

$$\rho = \exp(4.8679 - 0.42209x_1 - 34.369x_2 - 0.13265x_1^2 - 17.427x_1x_2 - 972.01x_2^2 - 0.0070277x_1^3 + 3.2692x_1^2x_2 + 135.54x_1x_2^2 + 6430.2x_2^3) \qquad \text{[g/ m}^3\text{]} \qquad (4)$$

Here $x_1 = \ln z$ and $x_2 = \frac{1}{u_{10}}$, z is height and u_{10} is wind speed at 10 m height. The expression is valid for z varying from 0.03 to 4 m and wind speed varying from 10 to 25 m/s.

The atmospheric shear stress is approximated by the Reynolds stress to be

$$\tau_{\mathrm{Re}} = \rho_{air} \nu_t \left| \frac{d\bar{U}}{dz} \right| \qquad [\mathrm{N/m^2}] \qquad (5)$$

where ν_t is the eddy viscosity, ρ_{air} is the density of air and $\frac{d\bar{U}}{dz}$ is the vertical wind speed gradient (Stull,1997).

The flow pattern around a cube has been subject to wind tunnel studies by Martinuzzi and Tropea (1993). They describe a recirculation zone forming between the stagnation point on the upwind wall and the ground. The recirculation zone is deflected down the sides of the cube, creating a horseshoe shaped system of vortices. Downwind the reattachment point of the wake, another recirculation zone is formed. It is postulated that this downwind wake region is entraining air from the horseshoe vortex and pulling the sides of the vortex towards the axis of symmetry. Downwind the reattachment point of the wake, the horseshoe opens up and the wake expands rapidly.

Snowdrifting around obstacles has previously been calculated with a drift flux model (Bang et. al., 1994). The model, which is included in the flow solver Flow-3D, calculates the drift of one fluid phase through another, and is based on low relative velocity between the two phases. The relative velocity between the snow phase and the air is defined as

$$u_r = D_f f_1 f_2 \left(\frac{\rho_2 - \rho_1}{\rho_1} \right) \frac{1}{\rho} \nabla p \qquad [\mathrm{m/s}] \qquad (6)$$

Here ∇p is the pressure gradient, *f* is volume fraction, ρ is density and the subscripts *1* and *2* denotes the two different fluids. The total mixture density is $\rho = f_1 \rho_1 + f_2 \rho_2$. D_f is a coefficient related to the friction between the snow phase and the air.

Thiis and Gjessing (1999) showed the snowdrift pattern formed by saltating snow around cubical obstacles. On the basis of measurements of snowdrifts around 2.5m cubes with different rooftops, they assumed that the position of the upwind snowdrift of the cube is defined by the extension of the upwind recirculation zone. They also assumed that the maximum deposition of snow at the sides of the cubes is occurring where the wake expands, just downwind of the downwind

reattachment point. They propose that accumulation of snow is a function of both the concentration of snow in the air and the inverse of the surface shear stress, τ_0^{-1}. The reason why there is little or no snow accumulation in the downwind wake area when only saltation transport mode is present, is that the snow particles are ploughed to the sides by the buildings and only small amounts of snow is entrained in the downwind wake. The wind conditions in the experiment period is shown in figure 1 and the measured snowdrifts around the cubes is shown in figure 2.

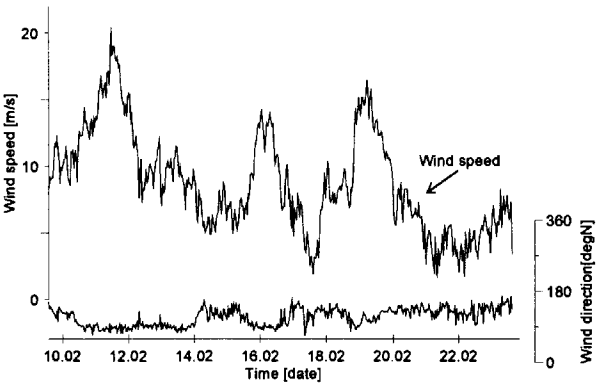

Fig. 1 Wind speed and direction in Adventdalen 09.02 - 23.02 1998

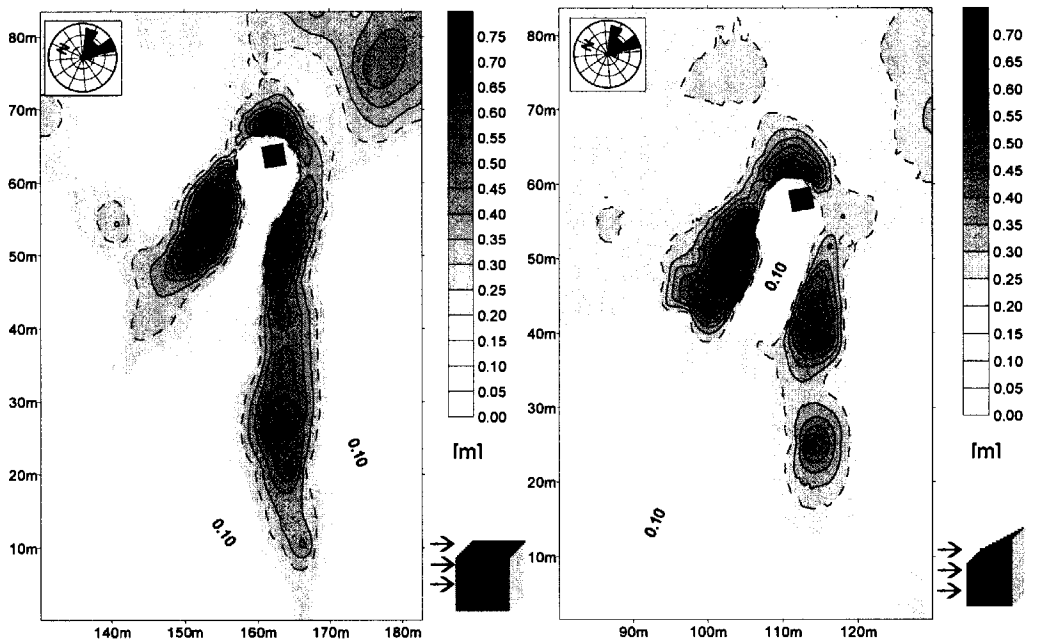

Fig. 2 a) Measured wind direction and snowdrifts around a flat roofed building. Fig. 2 b) Measured wind direction and snowdrifts around a single pitch roofed building with the highest wall away from the wind.

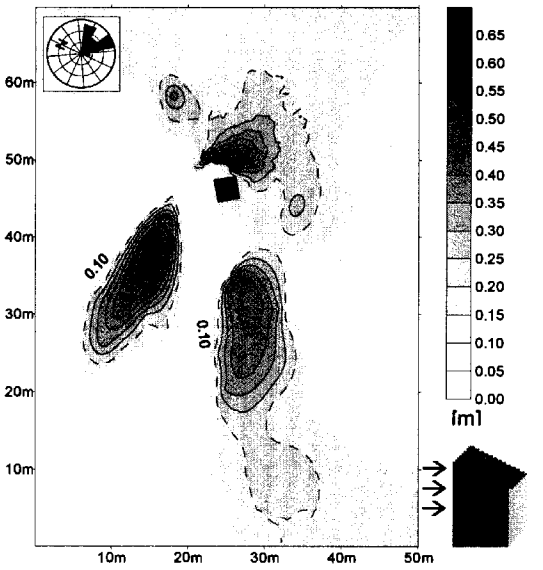

Fig. 2 c) Measured wind direction and snowdrifts around a single pitch roofed building with the highest wall against the wind.

METHODS

The airflow and snowdrifting around three square obstacles with different rooftops is calculated with a general purpose finite-volume CFD code (Flow 3D). The geometries are the same as Thiis and Gjessing (1999) used in their large scale measurements, with an incidence angle on the upwind wall equal to 25 degrees. The computational mesh is 95x60x15 m and consists of 76x74x25 cells with grid refinement near the cube.

The CFD code solves the incompressible, time averaged Navier-Stokes equations, using a k-ε turbulence model to close the equations. The k-ε model employs the eddy-viscosity concept, determining the eddy-viscosity, ν_t, from

$$\nu_t = C_\mu \frac{k^2}{\varepsilon} \qquad [\mathrm{m^2/s}] \qquad (7)$$

where C_μ is a constant equal to 0.09, k is turbulent kinetic energy and ε is the turbulent dissipation rate. Combining equations (5) and (7) gives the Reynolds stress, which in this case is approximating the atmospheric shear stress.

The inlet vertical wind velocity profile to the computational area follows the logarithmic expression

$$u(z) = \frac{u_*}{\kappa} \ln\left(\frac{z}{z_0}\right) \qquad \text{[m/s]} \tag{8}$$

where z is the height above the surface, z_0 is the roughness height, equal to 0.002 m, κ is the von karman constant equal to 0.4 and u_* is the friction velocity, equal to 0.6 m/s. This corresponds to a wind velocity of approximately 12 m/s at a 10 m height. The turbulence intensity on the inlet boundary is set to zero. This conserves the vertical wind profile through the computational area which is not affected by the cube. The outlet boundary is continuative, meaning that the normal derivatives of all quantities are set to zero. On the surface boundaries, a law-of-the wall velocity profile is assumed. The lateral and top boundaries have symmetry conditions.

For the snowdrifting simulations, the inlet snow density profile follows the profile suggested by Mellor and Fellers (1986) up to 0.5m. The snow particle density is set to 400 kg/m^3.

The friction coefficient in the drift flux model, D_f, is in this case found by balancing the drag force on a sphere with the buoyancy force, known as Stokes form of viscous flow about a sphere

$$D_f = \frac{2r_0^2}{9\nu} \tag{9}$$

where r_0 is the mean radius of the snow particles and ν is the kinematic viscosity of air. This is a valid assumption because of the low relative velocity between air and snow. The mean particle diameter is set to 0.25mm.

In the calculations, the density and the dynamic viscosity of air at –20 °C is set to 1.38 kg/m^3 and 1.63*10^{-5} N*s/m^2 respectively.

The apparent dynamic viscosity of the snow and air mixture is deduced from the threshold shear stress value for snow. Accumulation will occur in areas where atmospheric shear force on the surface is lower than the viscous forces of the snow. Since the threshold friction velocity when snowdrifting cease is known from measurements (Kind, 1981), a threshold shear stress and an apparent dynamic viscosity of the snow/air mixture μ_{app} can be determined

$$\tau_t = \rho_{air} u_{*t}^2 = \mu_{app} \frac{du}{dz}_{surface} \tag{10}$$

The vertical velocity gradient at the surface is found from the logarithmic expression for wind velocity with the friction velocity substituted with the chosen threshold friction velocity. The value for the

threshold friction velocity used in the calculations is 0.25 m/s. This results in an apparent dynamic viscosity of the snow and air mixture equal to μ_{app} =2.76*10^{-4} N*s/m^2.

RESULTS

Figure 3 shows a map of the atmospheric shear stress on the ground, deduced from equations (5) and (7). From this, it is evident that the cubes induces large low surface shear stress regions downwind of the cubes. Just upwind of the cubes there are local shear stress minima. These minima corresponds well to the border of the upwind recirculation zone, found from streamline visualisation, fig 4.

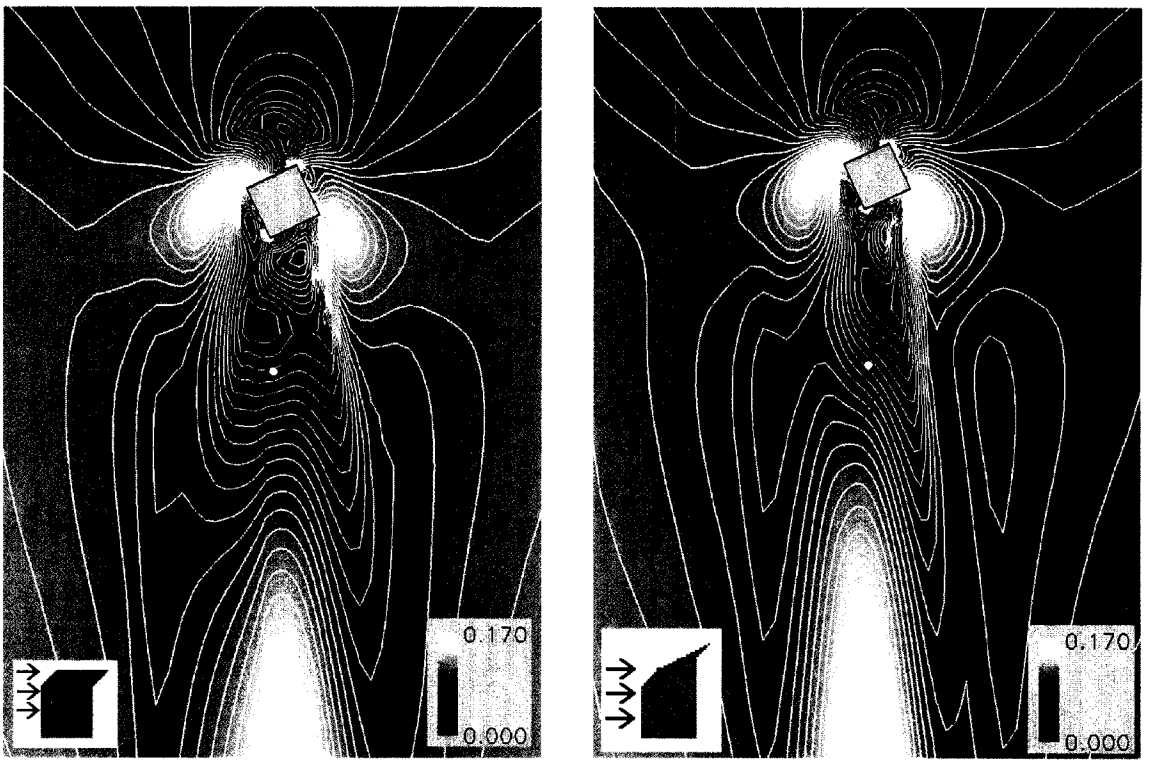

Figure 3. a) case a) calculated shear stress on the surface around a flat roofed building. The downwind reattachment point is indicated with a white dot, colour scale in N/m^2, contour line spacing is 7.7*10^{-3} N/m^2. b) case b) calculated shear stress around a single pitch roofed building with the highest wall away from the wind. The downwind reattachment point is indicated with a white dot, colour scale in N/m^2, contour line spacing is 7.7*10^{-3} N/m^2.

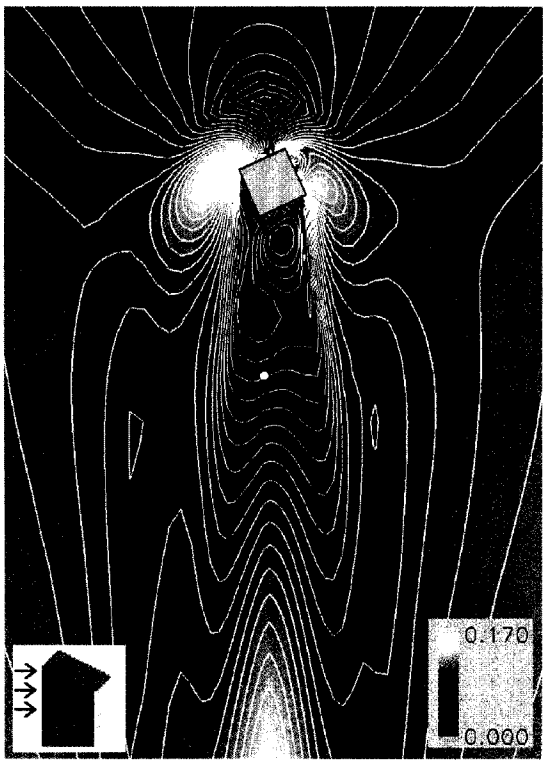

3. c) case c) calculated shear stress around a single pitch roofed building with the highest wall towards the wind. The downwind reattachment point is indicated with a white dot, colour scale in N/m^2, contour line spacing is $7.7*10^{-3}$ N/m^2.

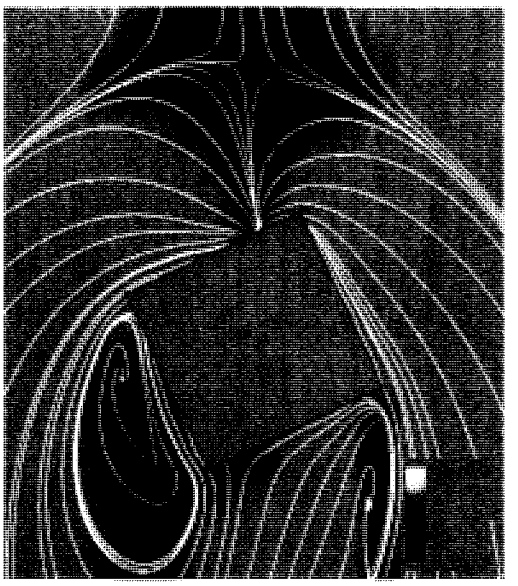

Figure 4. Calculated streamlines and surface shear stress around a single pitch roofed building with the highest wall away from the wind, colour scale in N/m^2.

The distance from the buildings to the upwind snowdrift, and the calculated distance from the building to the upwind local shear stress minimum is given in table 1. It can be seen that the variation in distance between the buildings and the upwind snowdrift is reasonably well computed, but that all the distances are somewhat overestimated. The reason for this might be that the turbulence model overestimates the turbulence in the calculations. This problem is usual for the k-ε turbulence model and is reported by Murakami (1993). The overestimation of the turbulence intensity might also influence the downwind wake by calculating too large reattachment zones.

Table 1. Extension of upwind recirculation zone

	Case A	Case B	Case C
Measured	1.6m	2.0m	2.5m
Computed	2.5m	2.8m	3.0m

The computations show that there is a local shear stress minimum on each side of the low shear stress zones downwind of the cubes. The downwind position of these minima are approximately equal to the location of the downwind reattachment points. The location of the reattachment point is found from a local pressure maximum, and is indicated with white dots in figure 3. These low surface shear stress zones displaced from the wake seems to correlate well with the position of the snowdrifts forming in the same area. Case a) has the zones positioned closest to the building, with the smallest distance between the zones, case b) further downwind, with a larger distance between the zones, and case c) has the zones positioned furthest away from the building, with the largest gap between them. The same variation is found in the large-scale measurements of the snowdrifts.

The calculations of snowdrifting around the obstacles reveal that the fluid fraction of the snow phase increases in the low shear stress zones upwind and on the sides of the buildings. The increased fluid fraction of snow increases the viscosity and the relative velocity between the two phases in these zones. This means that while the overall velocity of the air and snow is decreased because of a higher viscosity, the relative velocity between the phases is increased because of a higher fluid fraction of the snow phase. A higher relative velocity corresponds to a lower velocity of the snow phase and an increase of the local density. Figure 5 shows the height of the iso-surface of the fluid density ρ_f=1.396 kg/m^3.

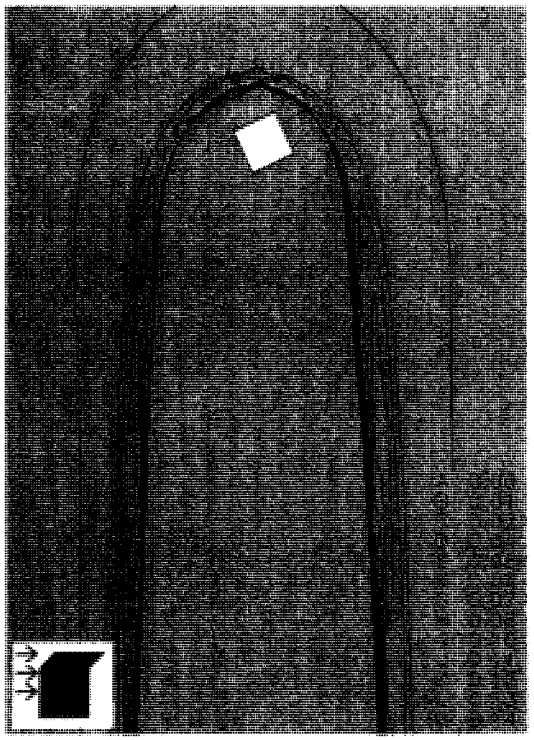

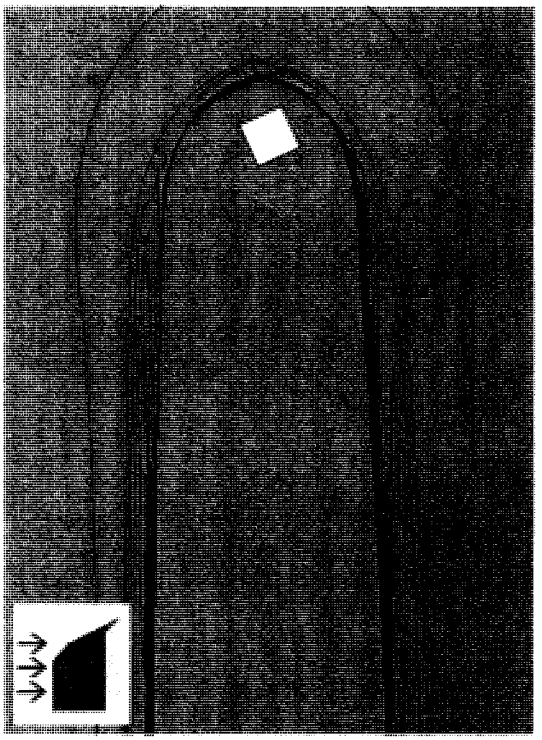

Figure 5 a) Calculated height of the iso-surface of fluid density ρ_f=1.396 kg/m^3 around a flat roofed building. Figure 5 b) Calculated height of the iso-surface of fluid density ρ_f=1.396 kg/m^3 around a single pitch roofed building with the highest wall away from the wind.

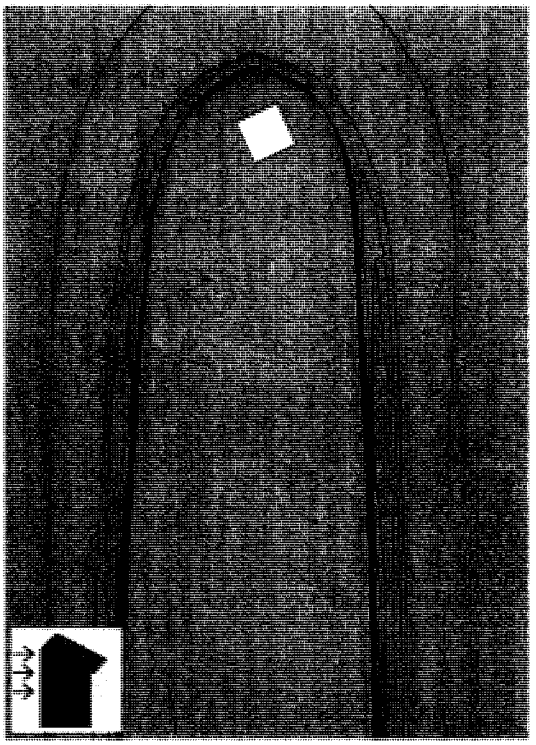

Figure 5 c) Calculated height of the iso-surface of fluid density ρ_f=1.396 kg/m^3 around a single pitch roofed building with the highest wall towards the wind.

It can be seen that the height of the iso-surfaces of the density is higher in the zones where snowdrift formation is expected. The variation of the position of these computed heights follows the pattern found from measurements. The upwind high density areas are positioned at the edge of the upwind recirculation zones, as the measurements expect. The maximum downwind snow density zones are positioned just downwind the downwind reattachment point. Between the lateral high density areas there is an area where the density is equal to the air density. This corresponds to observations of blowing snow being ploughed to the sides by the building. The relative size of the snowdrifts around the cubes can be suggested if one accept that there is a direct relationship between the height of the snowdrifts and the height of the iso-surfaces of the computed fluid density.

CONCLUDING DISCUSSION

The computed results of surface shear stress and snowdrifting show to a great extent agreement with the measurements. Both the downwind position and the asymmetry around the reattachment point have the same variations in the measured snowdrift pattern and the calculations. However, the measurements are results of several days of snowdrifting with slightly varying wind conditions, and a perfect correlation can not be expected. A varying upwind vertical wind speed gradient will have great effect on the size of the upwind recirculation zone, resulting in a smaller zone caused by a steeper gradient.

The accuracy of the wind pattern calculations is essential to compute a reliable snowdrift pattern. A lot of effort is put into this field of research, and more reliable turbulence models are being developed. Future calculations of the wind pattern close to solid obstacles does therefore have the potential to become more exact, thus making the computed snowdrift pattern more correct.

The method only determines the snowdrifting pattern around the buildings, and gives no new surface where the speed of the snow phase is set to zero. The snow phase is slowed down, thus increasing the density in the low shear stress regions around the buildings. To calculate the influence of the snowdrift geometry on the snow deposition, also a solidification model needs to be applied. Such model will probably produce lateral snowdrifts with a larger base area than what is suggested here, in that some of the blowing snow will be forced around the solidified snowdrifts and accumulate at the side of the snowdrifts. Field data of time dependent mass transport together with snowdrift

topography is required to calibrate such a solidification model and calculate the development rate of the snowdrifts. The current method can therefor only be employed to determine the position and the relative size of the expected snowdrifts.

On the basis of numerical simulations of wind and snowdrifting around cubical obstacles it is possible to reproduce measurements of the position of the snowdrifts forming around such obstacles during saltation transport with reasonable accuracy. The relative size of the snowdrifts can be estimated on the basis of the variation in height of an iso-surface of the fluid density. It is reasonable to assume that the calculation method can be applied also on other geometries with limited complexity.

REFERENCES

Bang, B., Nielsen, A., Sundsbø, P.A. and Wiik, T. (1994), "Computer Simulation of Wind Speed, Wind Pressure and Snow Accumulation around Buildings (SNOW-SIM)", *Energy and Buildings*, **21**, 235-243.

Flow Science Inc., (1997), "Flow 3D User's Manual", *Flow Science Inc., Los Alamos.*

Kind, R. J. (1981), "Snowdrifting", *Handbook of snow, Principles, Processes, Management and use*, pp. 338-359 Gray, D. M., Male, H. ed.

Mellor, M. and Fellers, G. (1986), "Concentration and Flux of Wind-blown Snow", US Army Corps of Engineers, Special Report 86-11.

Murakami, S. (1993), "Comparison of various turbulence models applied to a bluff body.", *J. Wind Eng. and Industrial Aerodynamics*, **46 & 47**. pp. 21-36.

Owen, P. R. (1964), "Saltation of uniform grains in air", *J. Fluid Mech.*, **20**, pp. 225-242.

Pomeroy, J. W., Gray, D.M. (1990), "Saltation of snow", *Water Resources Research*, **26**(7), pp 1583-1594.

Stull, R. B. (1997), *An Intoduction to Boundary Layer Meteorology,* Kluwer Academic Publishers, The Netherlands

Thiis, T. K., Gjessing, Y. (1999), "Large-Scale measurements of snowdrifts around flat roofed and single pitch roofed buildings", *Cold Reg. Science and Tech.*, in press.

0001
TI: A comparison of numerical simulations and full-scale measurements of snowdrifts around buildings
AU: Thiis, TK
SO: WIND AND STRUCTURES - ISSN: 1226-6116
vol. 3 , nr. 2 (2000) , s. 73-81
TY: Article
LA: English
SC: engineering, civil
construction & building technology
mechanics
KW: snowdrift
building
numerical simulation
cfd
wind
snow